Model Based Tissue Differentiation in MR Brain Images

Peter H. Mowforth and Jin Zhengping

The Turing Institute,
36 North Hanover Street,
Glasgow G1 2AD.

This paper describes a technique which establishes the correspondence between a magnetic resonance (MR) image of the brain and a model anatomical image. Following correspondence, it is demonstrated that segmentation of tissue types may be achieved along with the provision of medically relevant indexes for diagnosis.

The work reported in this paper is part of a project whose objective is the automated, model-based interpretation of medical images. A suggested overall structure of this system, see Fig. 1, involves descriptions at multi-

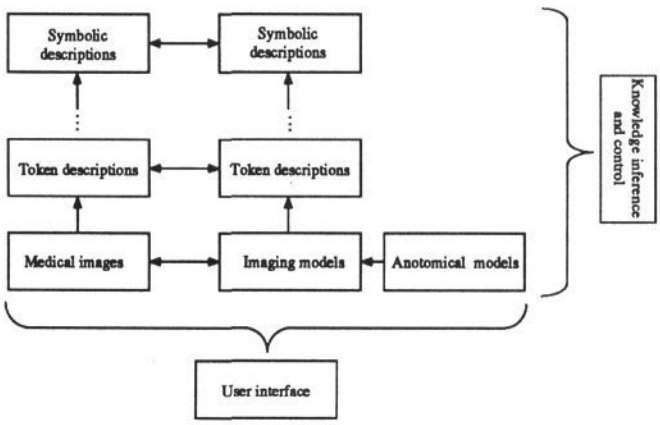

Figure 1: *Suggested overall framework for project.*

ple levels of abstraction. In order to interpret the medical images it is necessary to match them to anatomical models. Although this may be possible over a range of abstractions, the work reported here attempts correspondence only at the image level. Whilst the use of learning, symbolic reasoning and inference may be necessary for a complete system, this work explores how much can be achieved without such abstraction.

A MR machine has the ability to introduce contrast between tissue types on the basis of its imaging parameters. Given that the appearance of the resulting image is determined by the machine settings we require an imaging model for the machine. Such a model can be in the

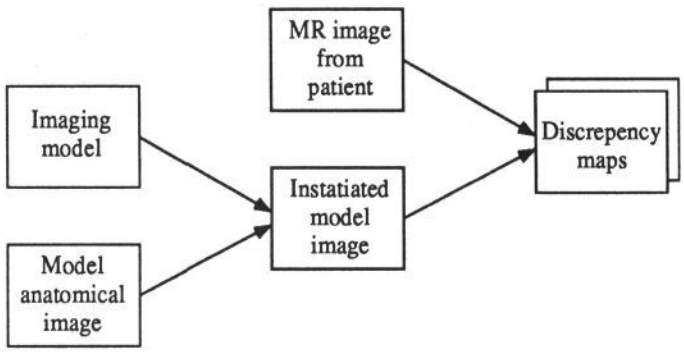

Figure 2: *Summary of the matching process which combines together a model anatomical image, an image from a patient using a MR scanner and the imaging model specific to that scanner.*

form of a look-up table providing contrast values for different machine settings and, if necessary, some estimate of their variation.

The first level of the anatomical model consists of image slices of a model brain for which the different tissues are represented by arbitrarily chosen gray values. These gray-valued variables may then be instantiated via the imaging model so as to produce an instantiated model image. The instantiated model image thus represents what we might expect a 'perfect' brain to look like under a certain set of machine protocols.

The final requirement is to match together the instantiated model image with the image derived from the patient. The discrepancies between the two may be represented via discrepancy maps. Fig. 2 shows a summary of this process.

Similar work using CT images of the brain has been described in [1]. Work which explored the usage of MRI to facilitate medical diagnosis and research has been reported in [9] where brain tissue MR images were classified by utilizing information such as gray levels and areas supplied by a head model. In [7] a general segmentation and recognition system has been 'instantiated' by encoding a domain-dependent subsystem of knowledge obtained through books and by interviewing experts to recognize MR brain images and PET brain images. Other relevant work has been reported in [10] where multispectral MRI and display techniques were used to obtain

AVC 1989 doi:10.5244/C.3.12

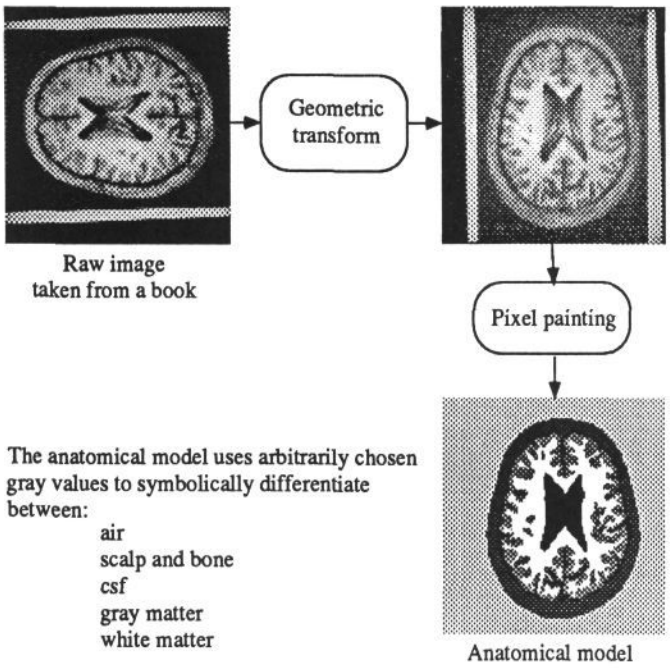

Figure 3: *Anatomical model building.*

higher contrast between tissue types of interest and background; in [8] where multispectral MRI has been used to provide a 'high information content' display which will aid in the diagnosis and analysis of the atherosclerotic disease process, and supervision of therapies; in [6] where MRI data have been used to reconstruct a 3D heart model which describes the shape of each part of the heart in a voxel space.

ANATOMICAL MODEL

The model anatomical image used in this paper is taken from the *Atlas of Sectional Human Anatomy* by J.G. Koritké and H. Sick [5]. The image in the atlas which corresponded to that captured from the patient was first digitised. A linear geometric transform was applied so as to compensate for the distortion introduced in the digitising process; *i.e.* the image was aligned vertically and centered.

The images were then hand-painted with arbitrarily chosen gray levels to symbolically differentiate between: background, scalp/bone, cerebro-spinal fluid (CSF), gray matter and white matter. These were chosen because they represent the tissue types primarily distinguished under MR protocols – see Fig. 3.

The anatomical model described is clearly the simplest that is of practical value. Work is already in progress to extend the model in two ways. First, multiple descriptions are necessary in order to code information such as anatomical regions (*e.g.* lobes) or anatomical structures (*e.g.* pons). Second, the model needs extending into a volumetric 3D form.

T_R[a]	T_E	GM	WM	CSF	B/S	Air
2000	100	115	84	171	18	3
2000	20	99	111	79	49	1
1080	100	107	79	132	19	3
1080	20	89	104	59	47	2

[a] Unit of T_R and T_E is *ms*.

Table 1: *An imaging model.*

IMAGING MODEL

The basic diagnostic indexes of MRI are the longitudinal (T_1) and transverse (T_2) proton (^{1}H) nuclear magnetic resonance (NMR) relaxation times of pathological human and animal tissues [2]. Whilst T_1 and T_2 are machine independent, MR machines typically only allow the user to specify two main control parameters. These are T_R and T_E. These are machine dependent and have a relation with T_1 and T_2 for a given tissue under some given condition. There is a further relation between T_1 and T_2 and the resulting gray values in the images produced by the machine. These gray values are machine dependent. An ideal imaging model should establish relations among T_1 and T_2, T_R and T_E, image gray levels, and other conditions such as temperature, species, and *in vivo* versus *in vitro* status.

To simplify the problem, this paper describes only the relationship between T_R and T_E and the tissue-dependent image gray levels.

The MR image derived from the patient uses a given pair of T_R and T_E values. The corresponding anatomical model image is instantiated by mapping each of its tissues to a particular gray level according to that relation. The machine dependent, instantiated model may now be used directly for matching.

Table 1 is an imaging model specific to a particular MR machine. To generate the imaging model we took 8 MR images of a human brain, using the same T_R and T_E values. The slices were 10mm thick and were separated by 10mm increments. Fig. 4 shows examples from one slice under four different control settings.

For each T_R and T_E and tissue type (including background), a sample of gray values were taken from that tissue type over all images at that T_R and T_E. The median values of each sample set were calculated and used to construct the imaging model shown in table 1.

INSTANTIATION OF THE ANATOMICAL MODEL

We may now instantiate the anatomical model with a range of T_R and T_E settings. For example, from the imaging model of Table 1, we obtain GM=115, WM=84, CSF=171, BONE/SCALP=18, AIR=3 through the index $T_R = 2000ms$, $T_E = 100ms$. These values were assigned to the corresponding tissues of the anatomical model image to instantiate it as seen in Fig. 5.

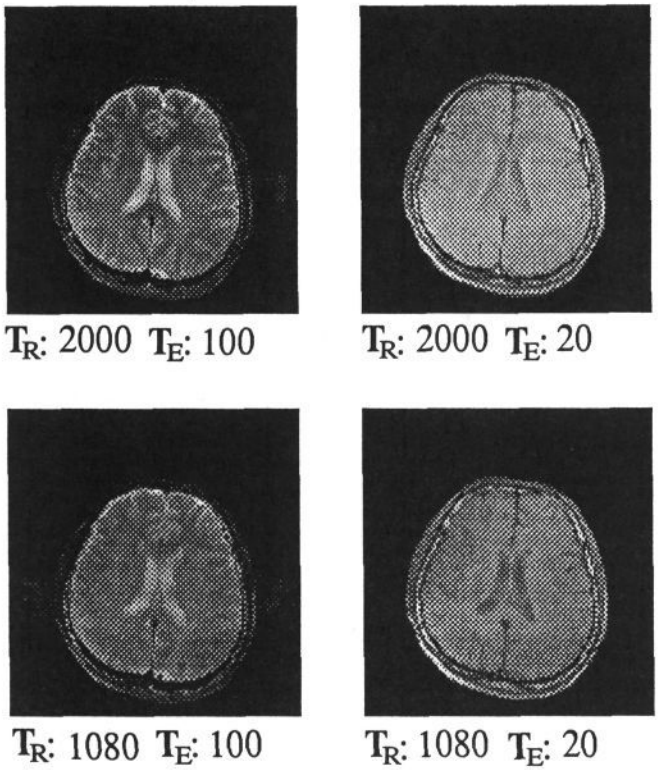

Figure 4: *MR images used in building the imaging model. 8 slices for each set of T_R and T_E.*

MATCHING

A MR image was taken from a patient using $T_R = 2000ms$ and $T_E = 100ms$ for approximately the same brain slice as shown in Fig. 5. Our goal is to match the image with that instantiated from the anatomical model. This is achieved as a two stage process. The first we call global matching where a global geometric transform is applied manually to rotate and stretch the image so as to bring it into approximate correspondence. The second stage, elastic matching, is an automatic process which establishes a continuous, sub-pixel correspondence between the two images.

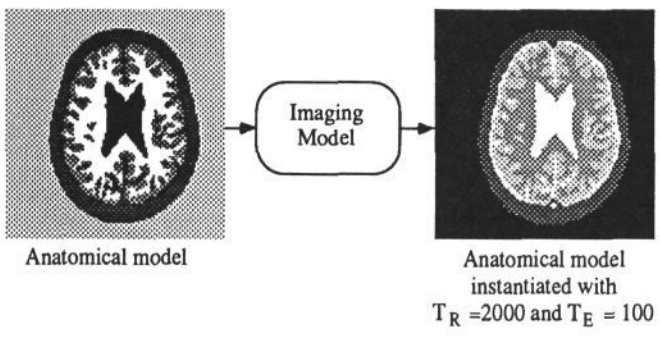

Figure 5: *Example instantiation of the anatomical model.*

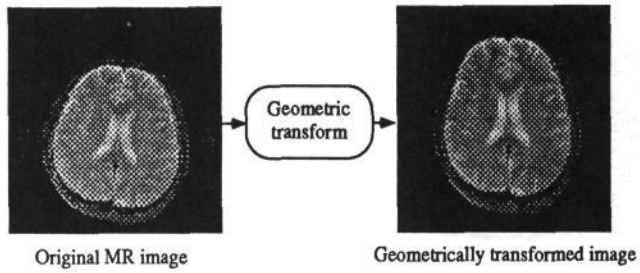

Figure 6: *Global matching.*

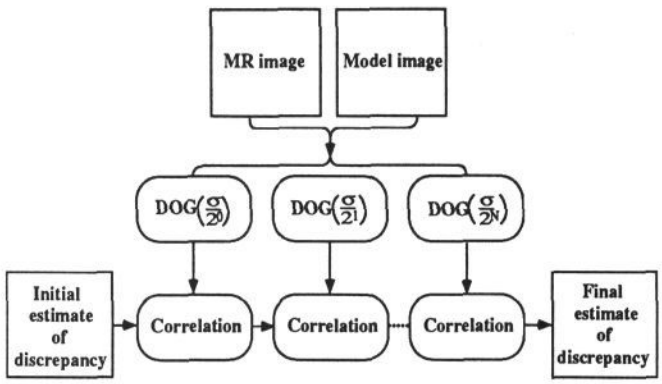

Figure 7: *Multiple scale matching.*

Global Matching

The position, orientation, size and aspect ratio of a MR image may differ from those of the anatomical model. To enable the matching process, a global transformation needs to be done which involves translation, rotation, scaling and elongation. This was carried out manually and the results are shown in Fig. 6.

Note that all of these transformations except the elongation are irrelevant to the variations of MR images from model images.

Elastic Matching

The geometric shapes of tissues are different among individuals. All brains are different and hence, the anatomical model can be viewed as a special (average) individual. The aim of the elastic matching is to measure all the discrepancies between the two special cases (the model and the patient).

The matching process used here is a multi-scale signal matcher(MSSM) [4]. It input is the globally matched image pair and its output is a pixel-by-pixel, continuous measure of all image discrepancies. Discrepancies are represented by two images, one which depicts all horizontal discrepancies and the other which depicts all vertical discrepancies.

Fig. 7 shows the software architecture for the multi-scale signal matching algorithm. Each of the two input images is blurred using a large $\nabla^2 G$ filter whose size is determined by σ. For each pixel in the model image,

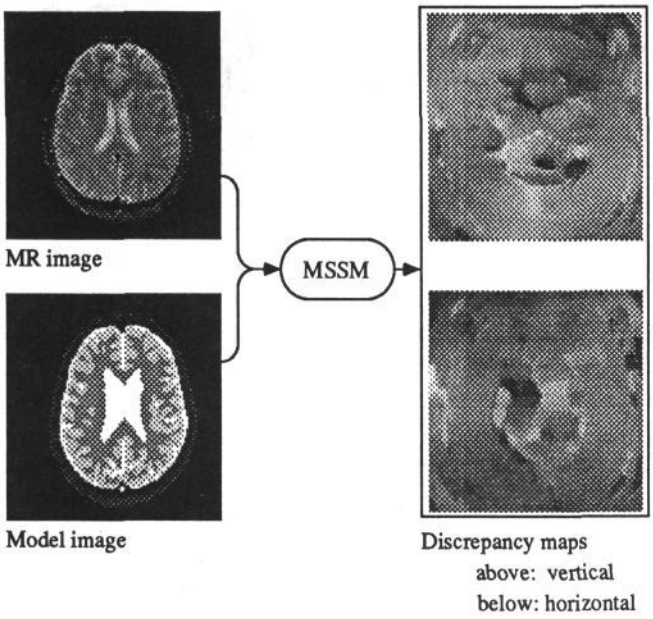

Figure 8: *Elastic matching of patient and model images.*

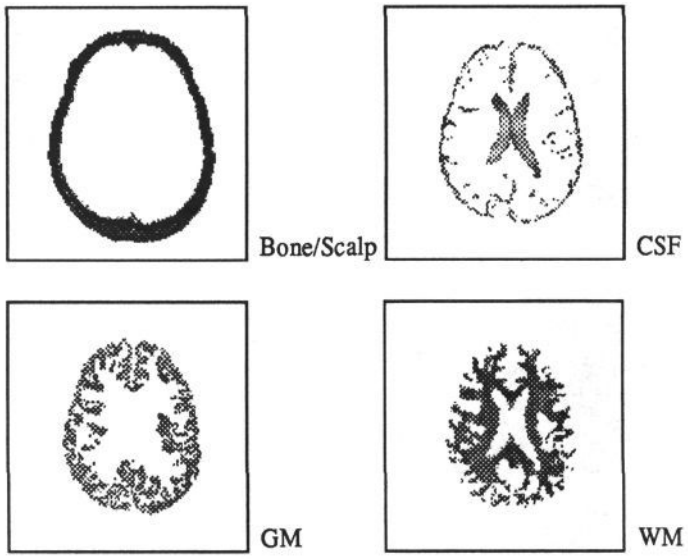

Figure 9: *Segmentation of the transformed MR image.*

the matching pixel in the medical image is searched for, using a cross-correlation function. The cross-correlation searches the neighbourhood of a pixel rather than a single pixel to provide the matching score. The search starts from the initial discrepancy estimate, *e.g.*, $(0,0)$ and ends at a local optimum around that initial discrepancy estimate. For the coarsest filter, the displacement of the pixel in the medical image is the initial discrepancy estimate for the algorithm. The output discrepancy maps (vertical and horizontal) are used as the initial discrepancy estimates for the input images convolved with a smaller $\nabla^2 G$ filter of $\sigma/2$. The process is repeated and so past through to finer scale filters following a coarse-to-fine regime. The output from the smallest filter is the final estimate of the image discrepancies.

RESULTS

The result of matching is shown in Fig. 8 with the gray values in the discrepancy maps providing a pixel-by-pixel measure of the magnitude of both the horizontal and vertical discrepancy.

Because a correspondence has now been established between the two, any knowledge available in the model image can be applied directly to the MR image. For example, we already know what tissue each pixel in the model image represents, hence we are immediately able to classify each pixel in the MR image. Fig. 9 shows the segmentation of each tissue type in the matched MR image.

Furthermore, since we knew the transformation we did in global matching, we can do the inverse transformation. Fig. 10 shows the segmented tissues following the inverse transformation which can be used directly to calculate the areas of each tissue type. Table 2 gives a summary of tissue type areas in pixels.

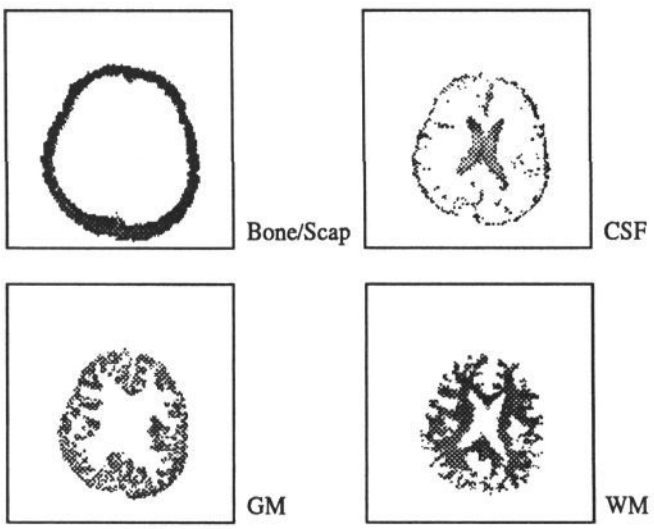

Figure 10: *Tissue segmentation for the original MR image.*

GM	WM	CSF	Bone/Scalp
1789	2100	967	1818

Table 2: *Area measurement of tissues in pixels.*

DISCUSSION

This experiment has demonstrated that, for a non-pathological MR image of a normal brain it is possible to perform tissue segmentation by direct matching at the image level. Such an approach may well prove sufficient for providing a simple diagnostic index. For example, in calculating ventricle volume which would facilitate the diagnosis of hydrocephalus [3].

ACKNOWLEDGEMENT

The authors thank Elizabeth Robinson at Picker International Company and Brian Dalton at GEC Hirst Laboratories for their assistance in capturing and supplying all the MR images necessary for this experiment. Thanks also to Alan Colchester at Guy's Hospital, London for his expertise and advice in model building; Douglas Scoular for help with providing the pixel painting software and the links between the Sun's and the Mac's. Finally, we acknowledge the valuable support offered to us by all the consortium members on the Alvey 134 project which sponsored this work.

References

[1] Ruzena Bajcsy and Stane Kovacic. Multiresolution elastic matching. *Computer Vision, Graphics, and Image Processing*, 46(1):1–21, 1989.

[2] P.A. Bottomley, C.J. Hardy, R.E. Argersinger, and G. Allen-Moore. A review of ^{1}H nuclear magnetic resonance relaxation in pathology: are T_1 and T_2 diagnostic? *Medical Physics*, 14(1):1–37, Jan/Feb 1987.

[3] B.R. Condon, J. Patterson, D. Wyper, D.M. Hadley, G. Teasdale, R. Grant, A. Jenkins, P. Macpherson, and J. Rowan. A quantitative index of ventricular and extraventricular intracranial CSF volumes using MR imaging. *Journal of Computer Assisted Tomography*, 10(5):784–792, September/October 1986.

[4] Z. Jin and P. Mowforth. *A discrete approach to signal matching.* Technical Report TIRM-88-036, The Turing Institute, Glasgow, Scotland, October 1988.

[5] J.G. Koritkié and II. Sick. *Atlas of Sectional Human Anatomy: Frontal, Sagittal, and Horizontal Planes.* Volume 1: Head, Neck, Thorax, Urban and Schwarzenberg, Baltimore-Munich, 1983.

[6] Michiyoshi Kuwahara and Shigeru Eiho. 3-D heart image reconstructed from MRI data. In *9th International Conference on Pattern Recognition*, pages 1198–1201, Computer Society Press, Rome, Italy, November 1988.

[7] Wei-Chung Lin, Yue-Tong Weng, and Chin-Tu Chen. Expert vision systems integrating image segmentation and recognition processes. *Engineering Applications of Artificial Intelligence*, 1(4):230–249, Dec. 1988.

[8] M.B. Merickel, C.S. Carmen, W.K. Watterson, J.R. Brookeman, and C.R. Ayers. Multispectral pattern recogniton of MR imagery for the noninvasive analysis of atherosclerosis. In *9th International Conference on Pattern Recognition*, pages 1192–1197, Computer Society Press, Rome, Italy, November 1988.

[9] Hidetomo Suzuki and Jun-ichiro Toriwaki. Knowledge-guided automatic thresholding for 3-dimesional display of head MRI images. In *9th International Conference on Pattern Recognition*, pages 1210–1212, Computer Society Press, Rome, Italy, November 1988.

[10] Michael W. Vannier, Christopher M. Speidel, Douglas L. Rickman, Larry D. Schertz, Lynette R. Baker, Charles F. Hildebolt, Carolyn J. Offutt, James A. Balko, Robert L. Butterfield, and Mokhtar H. Gado. Validation of magnetic resonance imaging (MRI) multispectral tissue classification. In *9th International Conference on Pattern Recognition*, pages 1182–1186, Computer Society Press, Rome, Italy, November 1988.